



Dynamical Evolution of Properties for Atom and Field in the Process of Two-Photon Absorption and Emission Between Atomic Levels

Jian-ming Wang^{1,2} · Xue-xiang Xu^{1,2}

Received: 19 December 2017 / Accepted: 26 March 2018 / Published online: 4 April 2018
© Springer Science+Business Media, LLC, part of Springer Nature 2018

Abstract Using dressed state method, we cleverly solve the dynamics of atom-field interaction in the process of two-photon absorption and emission between atomic levels. Here we suppose that the atom is initially in the ground state and the optical field is initially in Fock state, coherent state or thermal state, respectively. The properties of the atom, including the population in excited state and ground state, the atom inversion, and the properties for optical field, including the photon number distribution, the mean photon number, the second-order correlation function and the Wigner function, are discussed in detail. We derive their analytical expressions and then make numerical analysis for them. In contrast with Jaynes-Cummings model, some similar results, such as quantum Rabi oscillation, revival and collapse, are also exhibit in our considered model. Besides, some novel nonclassical states are generated.

Keywords Two-photon absorption and emission · Jaynes-Cummings model · Dressed state method · Atomic inversion · Wigner function

1 Introduction

Involving the atom-field interaction, one of the simplest and important problems, the coupling of a two-level atom with a single mode of the electromagnetic field, has aroused widespread interests of researchers for many years [1–9]. Because the two atomic levels are resonant or nearly resonant with the driving field (all other levels are highly detuned),

Project supported by the National Natural Science Foundation of China (No. 11665013).

✉ Xue-xiang Xu
xuxuexiang2005@163.com

¹ Center for Quantum Science and Technology, Jiangxi Normal University, Nanchang 330022, China

² College of Physics Communication Electronics, Jiangxi Normal University, Nanchang 330022, China

we can adopt a two-level atom description for the atom to deal with these problems [10–12]. Under certain realistic approximations, some problem can be reduced to a solvable form. Furthermore, some essential features will be extracted in the atom-field interaction. Representative solvable example is the Jaynes-Cummings model whose effective Hamiltonian is described by $\hbar\eta (a\sigma_+ + a^\dagger\sigma_-)$, where $a(a^\dagger)$ is the annihilation (creation) operator for the optical field, σ_+ (σ_-) is the raising (lowering) operator of the atom, and η is the coupling strength parameter [13, 14]. Some interesting phenomena for the atom, such as quantum Rabi oscillation and revival and collapse [15, 16], will exhibit after the atom-field interaction of the Jaynes-Cummings model. Moreover, some novel quantum states for optical fields will be prepared, which will satisfy the need of quantum state engineering and quantum technology [17]. Besides, there are many possible extensions of the original Jaynes-Cummings model involving various types of alternative interactions. For instance, some models, such as two-photon transitions, multimode and multilevel models, Raman coupled models, two-channel models etc. are involving among them [18–20].

In this paper, we consider a model of two-photon absorption and emission between two atomic levels, whose Hamiltonian is described effectively by $\hbar\eta (a^2\sigma_+ + a^{\dagger 2}\sigma_-)$ [1, 4]. In this process, the atoms in the excited state $|e\rangle$ make a transition to the lower level $|g\rangle$ by emitting two photons of frequency ν via a virtual level, where the phenomena happen at exact resonance ($\omega_{eg} = 2\nu$) and a single-mode two-photon laser can be generated. Fortunately, this is also an exact solvable model. Following the routines used in the Jaynes-Cummings model, we make a detailed investigation for our considered model. Our model will exhibit some similar results obtained from Jaynes-Cummings model, with proper parameter adjustment. One can resort to many different but equivalent methods to solve for the evolution of the atom-field system. These methods are often based on the solutions of the probability amplitudes, the Heisenberg operators, and the unitary time-evolution operator [21]. If the evolution of the system is unitary, the unitary time-evolution operator method is perhaps the simplest one among these methods. Furthermore, the eigenstates for our considered Hamiltonian are easy to find, which can help us to obtain the unitary evolution results. These eigenstates are called the “dressed” states [22]. Therefore, the method we used here is called the dressed-state method. This is appropriate to our present system.

The paper is organized as follows. In Section 2, the considered theoretical model and the dressed-state method to solve this model are introduced. In Section 3, we make a brief review of the related properties for the atom and the field. In Sections 4, 5 and 6, we study the dynamical behavior for the atom and the field under the three cases of initial conditions, i.e., assuming that the atom is initially in the ground state and the field is initially in the Fock state, the coherent state, and the thermal state, respectively. For every properties, we give their explicit expressions and make numerical simulations. Conclusions are summarized in the last section.

2 Theoretical Model and Dressed State Method

The effective Hamiltonian representing two-photon absorption and emission between two-level atom can be given by

$$H_{eff} = \hbar\eta (a^2\sigma_+ + a^{\dagger 2}\sigma_-), \quad (1)$$

where we think it as a resonant two-photon extension of the Jaynes-Cummings model in view of their similarity. In terms of the field number states, the interaction term in H_{eff} causes only transitions of the types

$$|e, n\rangle \leftrightarrow |g, n + 2\rangle. \tag{2}$$

The production states $|e, n\rangle, |g, n + 2\rangle$ ($n \geq 0$) are sometimes referred as the “bare” states, who are product states of the unperturbed atom and field. For a fixed n , the dynamics is completely confined to the two-dimensional Hilbert space $H^{(n)}$ ($n \geq 0$, also $n + 2 \geq 2$) of product states, i.e. $|e, n\rangle, |g, n + 2\rangle$. Obviously, $|e, n\rangle$ and $|g, n + 2\rangle$ are orthogonal. Using this basis in the 2×2 subspace, we obtain the matrix representation of H_{eff} ,

$$H_{eff} = \begin{pmatrix} 0 & \hbar\eta\sqrt{(n+2)(n+1)} \\ \hbar\eta\sqrt{(n+2)(n+1)} & 0 \end{pmatrix}. \tag{3}$$

This matrix is “self-contained” since the dynamics connects only those states for which the photon number changes by ± 2 . For the cases $|g, 0\rangle$ or $|g, 1\rangle$, we find that $H_{eff} |g, 0\rangle = 0$ and $H_{eff} |g, 1\rangle = 0$, which are the special point in our considered model.

For a given n , the energy eigenvalues of $H_{eff}^{(n)}$ are as follows

$$E_+^{(n)} = \eta\hbar\sqrt{(n+1)(n+2)}, \quad E_-^{(n)} = -\eta\hbar\sqrt{(n+1)(n+2)}. \tag{4}$$

The eigenstates $|\psi_+^{(n)}\rangle$ ($|\psi_-^{(n)}\rangle$) associated with the energy eigenvalues $E_+^{(n)}$ ($E_-^{(n)}$), satisfying the following eigen equation

$$H_{eff} |\psi_+^{(n)}\rangle = E_+^{(n)} |\psi_+^{(n)}\rangle, \quad H_{eff} |\psi_-^{(n)}\rangle = E_-^{(n)} |\psi_-^{(n)}\rangle, \tag{5}$$

are given by in the dressed state basis

$$\begin{aligned} |\psi_+^{(n)}\rangle &= \frac{1}{\sqrt{2}} |e, n\rangle + \frac{1}{\sqrt{2}} |g, n + 2\rangle, \\ |\psi_-^{(n)}\rangle &= \frac{1}{\sqrt{2}} |e, n\rangle - \frac{1}{\sqrt{2}} |g, n + 2\rangle, \end{aligned} \tag{6}$$

which can be recast back into the more familiar “bare” state basis

$$\begin{aligned} |e, n\rangle &= \frac{1}{\sqrt{2}} |\psi_+^{(n)}\rangle + \frac{1}{\sqrt{2}} |\psi_-^{(n)}\rangle, \\ |g, n + 2\rangle &= \frac{1}{\sqrt{2}} |\psi_+^{(n)}\rangle - \frac{1}{\sqrt{2}} |\psi_-^{(n)}\rangle. \end{aligned} \tag{7}$$

The variation of the dressed energies as a function of η is represented in Fig. 1. The dressed energies ($E_+^{(n)}$ and $E_-^{(n)}$) are the linear functions of the interaction parameter η with the respective slope $\pm\hbar\sqrt{(n+1)(n+2)}$ for different n . For no interaction $\eta = 0$, the energy $E_+^{(n)} = E_-^{(n)} = 0$.

Using the dressed-state method, the exact solution to the atom-field interaction problem can be obtained cleverly. This process has the following steps: (1) Expanding the initial density operator into the bare-state form and then changing it into the dressed-state form; (2) Operating the unitary operator (related to the effective Hamiltonian) on the initial density operator and obtaining the evolved density operator in the dressed-state form; (3) Recasting the evolved density operator back into the bare-state form and obtaining the total atom-field density operator at arbitrary time.

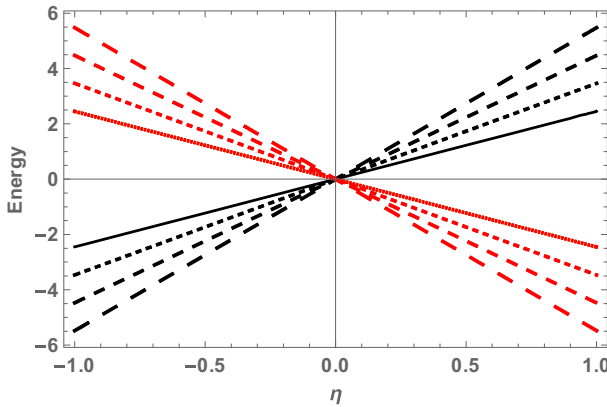


Fig. 1 (Color online) Dressed state energies as a function of the atom-field interaction parameter η . $E_+^{(n)}$ and $E_-^{(n)}$ are represented as black lines and red lines with different $n = 1, 2, 3, 4$

3 Properties for the Atom and the Optical Field

The total atom-field density operator $\rho_{AF}(t)$ at arbitrary time can be obtained after making the unitary operator $\exp(-\frac{i}{\hbar}H_{eff}t)$ on the initial density operator $\rho_{AF}(0)$, that is

$$\rho_{AF}(t) = \exp\left(-\frac{i}{\hbar}H_{eff}t\right)\rho_{AF}(0)\exp\left(\frac{i}{\hbar}H_{eff}t\right). \tag{8}$$

Hence, all the physically relevant quantities to the quantized field and the atom can be obtained from the density operator $\rho_{AF}(t)$. In other words, this total density operator will give us a complete description of our considered dynamical behavior.

3.1 For Atom

The reduced density operator of the atom is found by tracing over the field state

$$\rho_A(t) = \text{Tr}_F \rho_{AF}(t). \tag{9}$$

From (9), we can obtain the expressions

$$P_e(t) = \langle e | \rho_A(t) | e \rangle, P_g = \langle g | \rho_A(t) | g \rangle, \tag{10}$$

which represent the probabilities (or populations) that, at time t , the atom is in levels $|e\rangle$ and $|g\rangle$, respectively. Another important quantity is the atomic inversion, related to $P_e(t)$ and $P_g(t)$ by the expression

$$W(t) = P_e(t) - P_g(t), \tag{11}$$

where it is satisfied the condition $P_e(t) + P_g(t) = 1$.

3.2 For Field

Tracing over the atomic states, we obtain the reduced density operator of the field

$$\rho_F(t) = \text{Tr}_A \rho_{AF}(t). \tag{12}$$

In order to exhibit the characteristic of the evolved optical fields, we discuss their properties, including the photon number distribution, the mean photon number, the second-order

correlation function and the Wigner function in this paper. Next we make a brief introduction for these properties.

3.2.1 Photon Number Distribution

The probability $p_{n_p}(t)$, that there are n_p photons in the optical field at time t , is given as

$$P_{n_p}(t) = \langle n_p | \rho_F(t) | n_p \rangle, \tag{13}$$

i.e. photon number distribution, which must satisfy $\sum_{n_p=0}^{\infty} p_{n_p}(t) = 1$.

3.2.2 Mean Photon Number and Second-Order Correlation Function

The mean photon number and second-order correlation function of the optical field are given by

$$\langle n \rangle = \langle a^\dagger a \rangle \tag{14}$$

and

$$g^{(2)} = \frac{\langle a^{\dagger 2} a^2 \rangle}{\langle a^\dagger a \rangle^2}, \tag{15}$$

respectively [23]. The effect is antibunching when $g^{(2)} < 1$ (strictly nonclassical), and bunching (superbunching) if $1 \leq g^{(2)}(0) \leq 2$ ($g^{(2)}(0) > 2$). Obviously, $g^{(2)} = 1$ (Poissonian statistics) for a coherent state $|\alpha\rangle$; $g^{(2)} = 2$ for a thermal state; and $g^{(2)} = 0$ when $n = 0, 1$ and $g^{(2)} = 1 - 1/n$ when $n \geq 2$ for Fock state $|n\rangle$.

3.2.3 Wigner Function

In order to obtain a phase space distribution for a quantum particle, Wigner proposed firstly a function (i.e. Wigner function) in 1932, which is resembling as closely as possible the probability distribution of classical statistical physics [24]. The Wigner function of the optical field ρ_F at the point in phase space is

$$WF(\xi) = \frac{2}{\pi} \left\langle : \exp \left(-2 \left(a^\dagger - \xi^* \right) \left(a - \xi \right) \right) : \right\rangle, \tag{16}$$

whose complex-number coordinate is $\xi = (x + iy) / \sqrt{2}$. The integral of the Wigner function over phase space is equal to 1. Moreover, the Wigner function can take negative values in regions of the phase space, which is a signature of non-classical behavior for the corresponding state.

It is well known that the density operator for any quantum state can be expressed the form in Fock state, i.e. $\rho_F = \sum_{n,m} p_{nm} |n\rangle \langle m|$ with $p_{nm} = \langle n | \rho_F | m \rangle$. Hence, in order to calculate the Wigner function for any quantum state, we firstly derive the Wigner function for the operator $|n\rangle \langle m|$, whose general expression can be written as

$$WF_{|n\rangle \langle m|}(\xi) = \frac{2}{\pi} \langle m | : \exp \left(-2 \left(a^\dagger - \xi^* \right) \left(a - \xi \right) \right) : | n \rangle \tag{17}$$

The detailed derivation process is in the [Appendix](#).

In fact, the situation is considerably simpler if initially the atom is in the excited state $|e\rangle$. However, in the next three sections of this paper, we assume that the atom is initially in the ground state $|g\rangle$. Moreover, we assume that the initial optical field is in the photon number state, the coherent state, and the thermal state, respectively.

4 Dynamics Evolution for Initial Case I: $|\psi(0)\rangle = |g, n\rangle$

Assuming the atom initially in the ground state $|g\rangle$ and the field initially in a Fock state $|n\rangle$, i.e.

$$|\psi(0)\rangle = |g, n\rangle, \quad (18)$$

then the state vector for times $t > 0$ is just given by

$$|\psi(t)\rangle = \exp\left(-\frac{i}{\hbar} H_{eff} t\right) |g, n\rangle. \quad (19)$$

For the cases with the initial state $|\psi(0)\rangle = |g, 0\rangle$ or $|\psi(0)\rangle = |g, 1\rangle$, we have

$$H_{eff} |g, 0\rangle = 0, \quad H_{eff} |g, 1\rangle = 0, \quad (20)$$

i.e. the eigenvalue in these cases is zero, and then

$$\begin{aligned} |\psi(t)\rangle_{|g,0\rangle} &= \exp\left(-\frac{i}{\hbar} H_{eff} t\right) |g, 0\rangle = |g, 0\rangle, \\ |\psi(t)\rangle_{|g,1\rangle} &= \exp\left(-\frac{i}{\hbar} H_{eff} t\right) |g, 1\rangle = |g, 1\rangle, \end{aligned} \quad (21)$$

leading to

$$\begin{aligned} \rho_{AF}(t) |_{n=0} &= \rho_{AF}(0) |_{n=0} = |g, 0\rangle \langle g, 0|, \\ \rho_{AF}(t) |_{n=1} &= \rho_{AF}(0) |_{n=1} = |g, 1\rangle \langle g, 1|. \end{aligned} \quad (22)$$

For cases $n \geq 2$, noticing (4), (5) and (6), we have

$$|\psi(t)\rangle = \frac{e^{-i\sqrt{n(n-1)}\eta t}}{\sqrt{2}} |\psi_+^{(n-2)}\rangle - \frac{e^{i\sqrt{n(n-1)}\eta t}}{\sqrt{2}} |\psi_-^{(n-2)}\rangle. \quad (23)$$

After recasting back into the more familiar “bare” state basis by simplify substituting $|\psi_{\pm}^{(n-2)}\rangle$ from (6), we have

$$|\psi(t)\rangle = -i \sin(\sqrt{n(n-1)}\eta t) |e, n-2\rangle + \cos(\sqrt{n(n-1)}\eta t) |g, n\rangle, \quad (24)$$

whose conjugate state is

$$\langle\psi(t)| = i \langle e, n-2| \sin(\sqrt{n(n-1)}\eta t) + \langle g, n| \cos(\sqrt{n(n-1)}\eta t). \quad (25)$$

Thus the total density operator $\rho_{AF}(t) |_{n \geq 2} = |\psi(t)\rangle \langle\psi(t)|$ can be further expressed as

$$\begin{aligned} \rho_{AF}(t) |_{n \geq 2} &= \sin^2(\sqrt{n(n-1)}\eta t) |e, n-2\rangle \langle e, n-2| + \cos^2(\sqrt{n(n-1)}\eta t) |g, n\rangle \langle g, n| \\ &+ i \frac{\sin(2\sqrt{n(n-1)}\eta t)}{2} |g, n\rangle \langle e, n-2| - i \frac{\sin(2\sqrt{n(n-1)}\eta t)}{2} |e, n-2\rangle \langle g, n|. \end{aligned} \quad (26)$$

4.1 Properties of Atom for Initial Case I

The reduced density operator of the atom is found

$$\rho_A(t) |_{n \geq 2} = \sin^2(\sqrt{n(n-1)}\eta t) |e\rangle \langle e| + \cos^2(\sqrt{n(n-1)}\eta t) |g\rangle \langle g|, \quad (27)$$

which leads to the populations of the excited and ground states,

$$P_e(t) |_{n \geq 2} = \sin^2(\sqrt{n(n-1)}\eta t), \quad P_g(t) |_{n \geq 2} = \cos^2(\sqrt{n(n-1)}\eta t), \quad (28)$$

respectively, and satisfying $P_e(t) + P_g(t) = 1$. The atomic inversion is given by

$$W(t)|_{n \geq 2} = -\cos(2\sqrt{n(n-1)}\eta t). \tag{29}$$

Noticing for the cases $n = 0$ or $n = 1$, we always have $P_e(t) = 0$, $P_g(t) = 1$, and $W(t) = -1$. These are cases for the n -photon inversion. In Fig. 2, we plot the populations ($P_e(t)$, $P_g(t)$) and the atomic inversion $W(t)$ as a function of the scaled time ηt for different initial n . Obviously, they are all strictly periodic functions of the evolution time ηt with a quantum Rabi frequency $2\sqrt{n(n-1)}$ (different from that frequency $2\sqrt{n}$ in the Jaynes-Cummings model) related to the different photon number n . The result shows that the behavior of the atomic dynamics for a definite number photons is periodic and regular in our present model.

4.2 Properties of Field for Initial Case I

For cases $n = 0$ or $n = 1$, we have $\rho_F(t)|_{n=0} = |0\rangle\langle 0|$ and $\rho_F(t)|_{n=1} = |1\rangle\langle 1|$, which is independent of the evolution time. While for cases $n \geq 2$, the density operator of the optical field is

$$\rho_F(t)|_{n \geq 2} = \sin^2(\sqrt{n(n-1)}\eta t)|n-2\rangle\langle n-2| + \cos^2(\sqrt{n(n-1)}\eta t)|n\rangle\langle n|, \tag{30}$$

which is an incoherent superposition state of $|n-2\rangle\langle n-2|$ and $|n\rangle\langle n|$ with certain ratio depending on the evolution time.

4.2.1 Photon Number Distribution

The photon number distribution of the optical field evolved from initial case I has the following characteristics. If $n = 0$, then we have

$$P_0(t) = 1, P_{n_p}(t) = 0(n_p \geq 1). \tag{31}$$

Similarly, if $n = 1$, then we have

$$P_1(t) = 1, P_{n_p}(t) = 0(n_p = 0 \text{ and } n_p \geq 2). \tag{32}$$

Obviously, if the field is initially in $|0\rangle$ or $|1\rangle$, it will remain in its original state forever.

But when $n \geq 2$, we have

$$\begin{aligned} P_{n-2}(t) &= \sin^2(\sqrt{n(n-1)}\eta t), & P_n(t) &= \cos^2(\sqrt{n(n-1)}\eta t), \\ P_{n_p}(t) &= 0 \quad (n_p \neq n-2 \text{ and } n). \end{aligned} \tag{33}$$

In Fig. 3, we plot P_{n_p} versus n_p for different number n at different time ηt . For a given initial Fock state $|n\rangle$ ($n \geq 2$), it will evolve into two components (i.e., $|n-2\rangle$ and $|n\rangle$) with the certain ratios depending on the interaction.

4.2.2 Mean Photon Number and Second-Order Autocorrelation Function

For the evolved optical field in this initial case, we have

$$\begin{aligned} \langle a^\dagger a \rangle|_{n=0} &= 0, & \langle a^\dagger a \rangle|_{n=1} &= 1, \\ \langle a^\dagger a \rangle|_{n \geq 2} &= (n-2)\sin^2(\sqrt{n(n-1)}\eta t) + n\cos^2(\sqrt{n(n-1)}\eta t), \end{aligned} \tag{34}$$

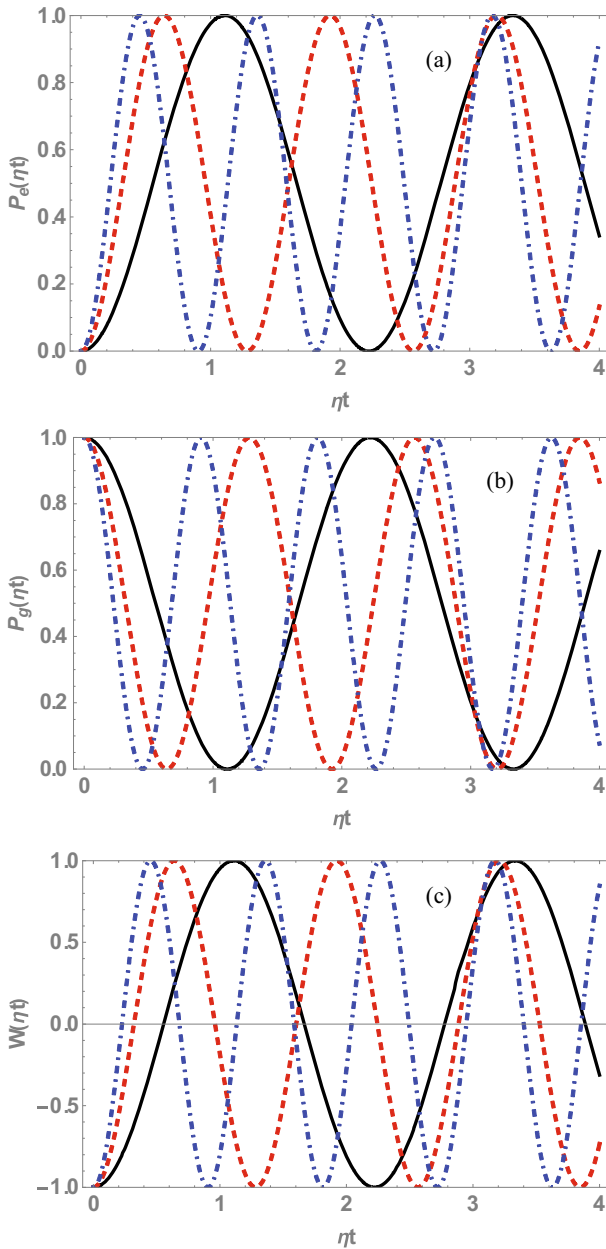


Fig. 2 (Color online) (a) Population in the excited state P_e , (b) Population in the ground state P_g , and (c) Atomic inversion W as a function of the time ηt , respectively, where atom is initially in the ground state $|g\rangle$ and the field is initially in a number state $|n\rangle$, and $n = 2, 3, 4$ are corresponding to the black solid, red dashed, and blue dot-dashed line, respectively

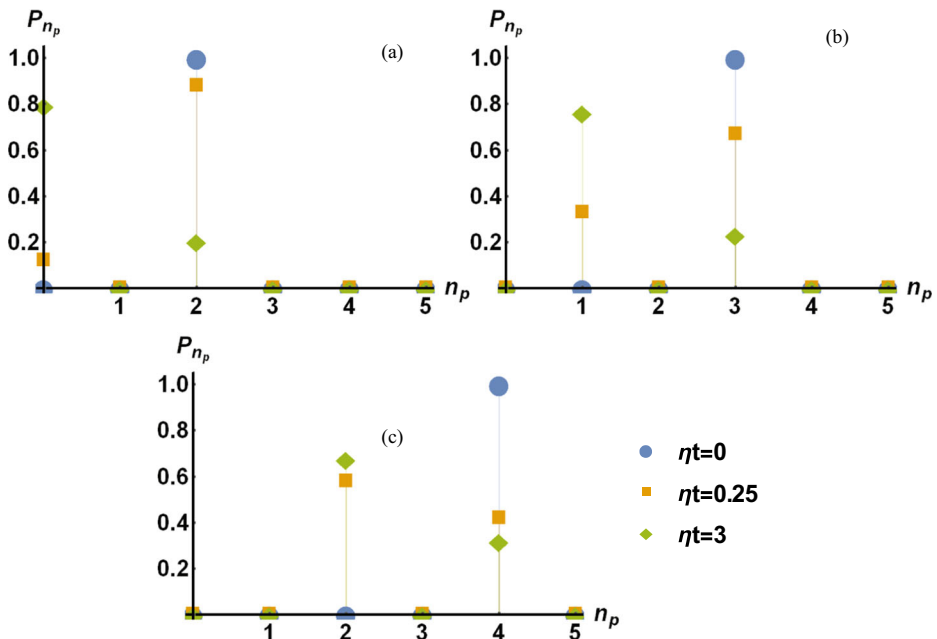


Fig. 3 (Color online) Evolution of photon number distribution P_{n_p} at time $\eta t = 0, 0.25, 3$ when (a) $n = 2$, (b) $n = 3$, (c) $n = 4$, respectively, where atom is initially in the ground state $|g\rangle$ and the field is initially in a number state $|n\rangle$

and

$$\langle a^{\dagger 2} a^2 \rangle|_{n=0} = 0, \quad \langle a^{\dagger 2} a^2 \rangle|_{n=1} = 0,$$

$$\langle a^{\dagger 2} a^2 \rangle|_{n \geq 2} = (n - 2)(n - 3) \sin^2(\sqrt{n(n - 1)}\eta t) + n(n - 1) \cos^2(\sqrt{n(n - 1)}\eta t) \quad (35)$$

Obviously, $\langle a^\dagger a \rangle$ remains unchanged for $n = 0, 1$, but is periodic function of ηt when $n \geq 2$ (see Fig. 4a). In addition, for $n = 0, 1$, $g^{(2)}$ is still zero; but when $n \geq 2$, $g^{(2)}$ is not always equal to $1 - 1/n$, but depends on n and ηt , as shown in Fig. 4b.

4.2.3 Wigner Function

The Wigner function of the Fock state $|n\rangle$ can be expressed as

$$WF(\xi) = \frac{2}{\pi} (-1)^n L_n(4|\xi|^2) \exp(-2|\xi|^2). \quad (36)$$

It is a non-Gaussian function in the form because of the existence of the Laguerre function, except the vacuum state $|0\rangle$.

Using (17), we obtain the time evolution of the Wigner function in this case expressed as

$$\begin{aligned} WF(\xi, t)|_{n=0} &= WF_{|0\rangle\langle 0|}(\xi), \quad WF(\xi, t)|_{n=1} = WF_{|1\rangle\langle 1|}(\xi), \\ WF(\xi, t)|_{n \geq 2} &= \sin^2(\sqrt{n(n - 1)}\eta t) WF_{|n-2\rangle\langle n-2|}(\xi) + \cos^2(\sqrt{n(n - 1)}\eta t) WF_{|n\rangle\langle n|}(\xi). \end{aligned} \quad (37)$$

As shown in Fig. 5, the Wigner function is symmetrical in phase space and can take negative values in some regions.

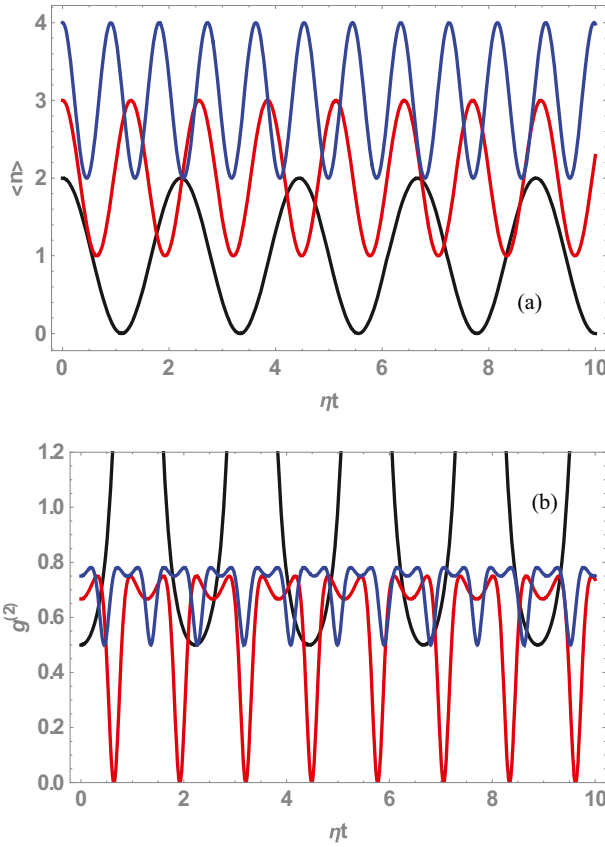


Fig. 4 (Color online) (a) Mean photon number and (b) second-order correlation function $g^{(2)}$ of the optical field as a function of the time ηt , where the field is initially in a number state $|n\rangle$, and $n = 2, 3, 4$ are corresponding to the black, red, and blue line, respectively

5 Dynamics Evolution for Initial Case II: $|\psi(0)\rangle = |g, \alpha\rangle$

Assuming the atom initially in the ground state $|g\rangle$ and the field initially in a coherent state $|\alpha\rangle$. Since the coherent state can be expanded as $|\alpha\rangle = \sum_{n=0}^{\infty} C_n |n\rangle$ with the coefficient $C_n = e^{-|\alpha|^2/2} \alpha^n / \sqrt{n!}$, then the initial state vector

$$|\psi(0)\rangle = \sum_{n=0}^{\infty} C_n |g, n\rangle, \tag{38}$$

will evolve into the state vector

$$|\psi(t)\rangle = \sum_{n=0}^{\infty} C_n \exp\left(-\frac{i}{\hbar} H_{eff} t\right) |g, n\rangle, \tag{39}$$

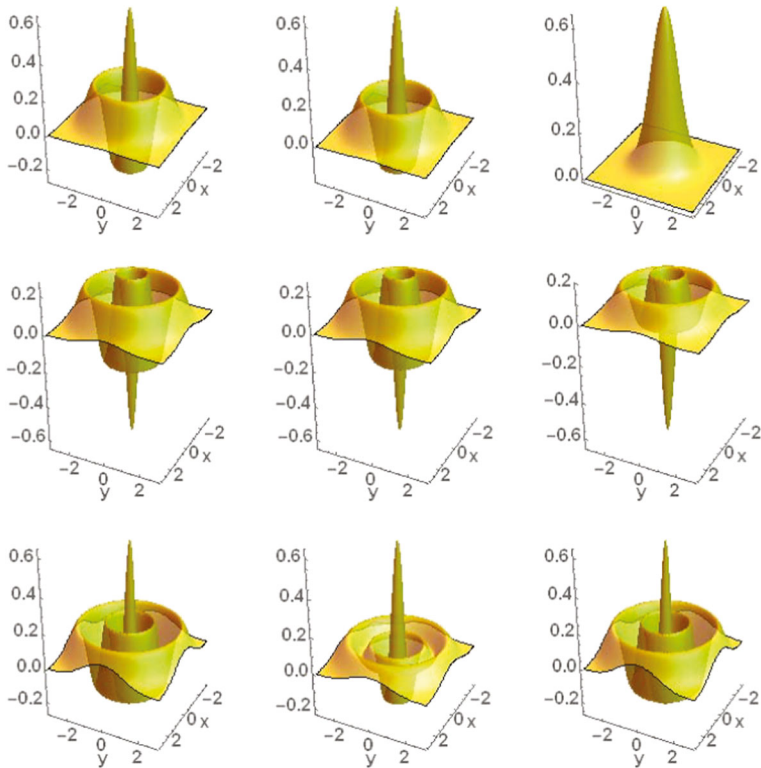


Fig. 5 (Color online) Wigner functions as a function of $\zeta = x + iy$ ($x, y \in [-3, 3]$) for quantum states $\rho_F(t) |_{n=2}$ (row 1), $\rho_F(t) |_{n=3}$ (row 2), and $\rho_F(t) |_{n=4}$ (row 3) and different time scales $\eta t = 0$ (column 1), 0.25 (column 2), and 10 (column 3), respectively

for times $t > 0$. Using the similar steps in above section, we have

$$\begin{aligned}
 |\psi(t)\rangle &= C_0 |g, 0\rangle + C_1 |g, 1\rangle \\
 &+ \sum_{n=2}^{\infty} C_n [-i \sin(\sqrt{n(n-1)}\eta t) |e, n-2\rangle + \cos(\sqrt{n(n-1)}\eta t) |g, n\rangle], \quad (40)
 \end{aligned}$$

with its corresponding conjugate state

$$\begin{aligned}
 \langle\psi(t)| &= C_0^* \langle g, 0| + C_1^* \langle g, 1| \\
 &+ \sum_{m=2}^{\infty} C_m^* [i \langle e, m-2| \sin(\sqrt{m(m-1)}\eta t) + \langle g, m| \cos(\sqrt{m(m-1)}\eta t)]. \quad (41)
 \end{aligned}$$

Thus the total density operator $\rho_{AF}(t) = |\psi(t)\rangle \langle \psi(t)|$ can be written as

$$\begin{aligned}
 \rho_{AF}(t) = & +C_0C_0^* |g, 0\rangle \langle g, 0| + C_0C_1^* |g, 0\rangle \langle g, 1| + C_1C_0^* |g, 1\rangle \langle g, 0| + C_1C_1^* |g, 1\rangle \langle g, 1| \\
 & +i \sum_{m=2}^{\infty} C_m^* C_0 \sin(\sqrt{m(m-1)}\eta t) |g, 0\rangle \langle e, m-2| + \sum_{m=2}^{\infty} C_m^* C_0 \cos(\sqrt{m(m-1)}\eta t) |g, 0\rangle \langle g, m| \\
 & +i \sum_{m=2}^{\infty} C_m^* C_1 \sin(\sqrt{m(m-1)}\eta t) |g, 1\rangle \langle e, m-2| + \sum_{m=2}^{\infty} C_m^* C_1 \cos(\sqrt{m(m-1)}\eta t) |g, 1\rangle \langle g, m| \\
 & -i \sum_{n=2}^{\infty} C_n C_0^* \sin(\sqrt{n(n-1)}\eta t) |e, n-2\rangle \langle g, 0| + \sum_{n=2}^{\infty} C_n C_0^* \cos(\sqrt{n(n-1)}\eta t) |g, n\rangle \langle g, 0| \\
 & -i \sum_{n=2}^{\infty} C_n C_1^* \sin(\sqrt{n(n-1)}\eta t) |e, n-2\rangle \langle g, 1| + \sum_{n=2}^{\infty} C_n C_1^* \cos(\sqrt{n(n-1)}\eta t) |g, n\rangle \langle g, 1| \\
 & + \sum_{n=2}^{\infty} \sum_{m=2}^{\infty} C_n C_m^* \sin(\sqrt{n(n-1)}\eta t) \sin(\sqrt{m(m-1)}\eta t) |e, n-2\rangle \langle e, m-2| \\
 & -i \sum_{n=2}^{\infty} \sum_{m=2}^{\infty} C_n C_m^* \sin(\sqrt{n(n-1)}\eta t) \cos(\sqrt{m(m-1)}\eta t) |e, n-2\rangle \langle g, m| \\
 & +i \sum_{n=2}^{\infty} \sum_{m=2}^{\infty} C_n C_m^* \cos(\sqrt{n(n-1)}\eta t) \sin(\sqrt{m(m-1)}\eta t) |g, n\rangle \langle e, m-2| \\
 & + \sum_{n=2}^{\infty} \sum_{m=2}^{\infty} C_n C_m^* \cos(\sqrt{n(n-1)}\eta t) \cos(\sqrt{m(m-1)}\eta t) |g, n\rangle \langle g, m|. \tag{42}
 \end{aligned}$$

5.1 Properties of Atom for Initial Case II:

The reduced density operator of the atom is

$$\begin{aligned}
 \rho_A(t) = & (|C_0|^2 + |C_1|^2) |g\rangle \langle g| \\
 & +i C_2^* C_0 \sin(\sqrt{2}\eta t) |g\rangle \langle e| - i C_2 C_0^* \sin(\sqrt{2}\eta t) |e\rangle \langle g| \\
 & +i C_3^* C_1 \sin(\sqrt{6}\eta t) |g\rangle \langle e| - i C_3 C_1^* \sin(\sqrt{6}\eta t) |e\rangle \langle g| \\
 & + \sum_{n=2}^{\infty} |C_n|^2 \sin^2(\sqrt{n(n-1)}\eta t) |e\rangle \langle e| + \sum_{n=2}^{\infty} |C_n|^2 \cos^2(\sqrt{n(n-1)}\eta t) |g\rangle \langle g| \\
 & -i \sum_{n=2}^{\infty} C_{n+2} C_n^* \sin(\sqrt{(n+1)(n+2)}\eta t) \cos(\sqrt{n(n-1)}\eta t) |e\rangle \langle g| \\
 & +i \sum_{n=2}^{\infty} C_n C_{n+2}^* \sin(\sqrt{(n+1)(n+2)}\eta t) \cos(\sqrt{n(n-1)}\eta t) |g\rangle \langle e|, \tag{43}
 \end{aligned}$$

leading to the populations of the excite and ground state

$$\begin{aligned}
 P_e(t) &= \sum_{n=2}^{\infty} |C_n|^2 \sin^2(\sqrt{n(n-1)}\eta t), \\
 P_g(t) &= |C_0|^2 + |C_1|^2 + \sum_{n=2}^{\infty} |C_n|^2 \cos^2(\sqrt{n(n-1)}\eta t). \tag{44}
 \end{aligned}$$

Here, we can verify that $P_e(t) + P_g(t) = 1$ and obtain the atom inversion

$$W(t) = - \sum_{n=2}^{\infty} |C_n|^2 \cos(2\sqrt{n(n-1)}\eta t) - |C_0|^2 - |C_1|^2. \tag{45}$$

The result is just the sum of n -photon inversion weighted with the photon number distribution of the initial coherent state. For convenience, we set $C_n = C_n^* = \sqrt{\frac{\bar{n}^n}{n!}} e^{-\bar{n}}$ for the coherent state $|\alpha\rangle$ with $\alpha = |\alpha| e^{i\theta} = \sqrt{\bar{n}} e^{i\theta}$ (\bar{n} denotes the mean photon number and let $\theta = 0$ here) in our following simulation.

Plots of $P_e(t)$, $P_g(t)$, $W(t)$ versus the scaled time ηt are shown in Fig. 6 for an initial coherent state with different \bar{n} . It is astonishing that their behaviors for an initial coherent state are quite different from that for an initial Fock state, i.e. quantum Rabi oscillations. Furthermore, for a moderate \bar{n} , the time evolution of the populations and the inversion shows the well-known collapse and revival.

5.2 Properties of Field for Initial Case II

The reduced density operator of the field is

$$\begin{aligned} \rho_F(t) = & |C_0|^2 |0\rangle \langle 0| + C_0 C_1^* |0\rangle \langle 1| + C_1 C_0^* |1\rangle \langle 0| + |C_1|^2 |1\rangle \langle 1| \\ & + \sum_{n=2}^{\infty} C_n C_0^* \cos(\sqrt{n(n-1)}\eta t) |n\rangle \langle 0| + \sum_{n=2}^{\infty} C_n^* C_0 \cos(\sqrt{n(n-1)}\eta t) |0\rangle \langle n| \\ & + \sum_{n=2}^{\infty} C_n C_1^* \cos(\sqrt{n(n-1)}\eta t) |n\rangle \langle 1| + \sum_{n=2}^{\infty} C_n^* C_1 \cos(\sqrt{n(n-1)}\eta t) |1\rangle \langle n| \\ & + \sum_{n=2}^{\infty} \sum_{m=2}^{\infty} C_n C_m^* \sin(\sqrt{n(n-1)}\eta t) \sin(\sqrt{m(m-1)}\eta t) |n-2\rangle \langle m-2| \\ & + \sum_{n=2}^{\infty} \sum_{m=2}^{\infty} C_n C_m^* \cos(\sqrt{n(n-1)}\eta t) \cos(\sqrt{m(m-1)}\eta t) |n\rangle \langle m|. \end{aligned} \tag{46}$$

5.2.1 Photon Number Distribution

The photon number distribution for this case can be described as follows

$$\begin{aligned} P_0(t) &= |C_0|^2 + |C_2|^2 \sin^2(\sqrt{2}\eta t), \\ P_1(t) &= |C_1|^2 + |C_3|^2 \sin^2(\sqrt{6}\eta t), \\ P_{n_p}(t) &= |C_{n_p}|^2 \cos^2(\sqrt{n_p(n_p-1)}\eta t) \\ &\quad + |C_{n_p+2}|^2 \sin^2(\sqrt{(n_p+1)(n_p+2)}\eta t), \\ &\quad (n_p \geq 2). \end{aligned} \tag{47}$$

In Fig. 7, we plot $P_{n_p}(t)$ for an initial coherent state. As \bar{n} increases, the distribution is wider. Moreover, some oscillation will exhibit at certain time.

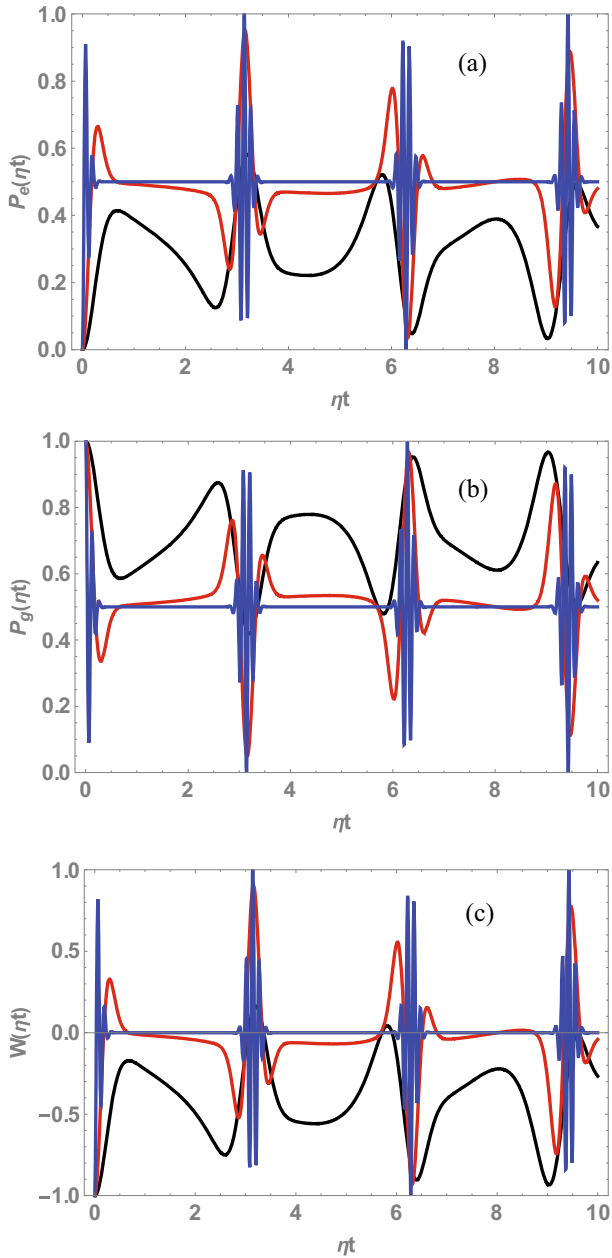


Fig. 6 (Color online) **(a)** Population in the excited state P_e , **(b)** population in the ground state P_g , **(c)** Atomic inversion W as a function of the time ηt , respectively, where atom is initially in the ground state $|g\rangle$ and the field is initially in a coherent state $|\alpha\rangle$ with $|\alpha| = \sqrt{\bar{n}}$ ($\bar{n} = 2, 5, 25$ are corresponding to the black, red, and blue line, respectively)

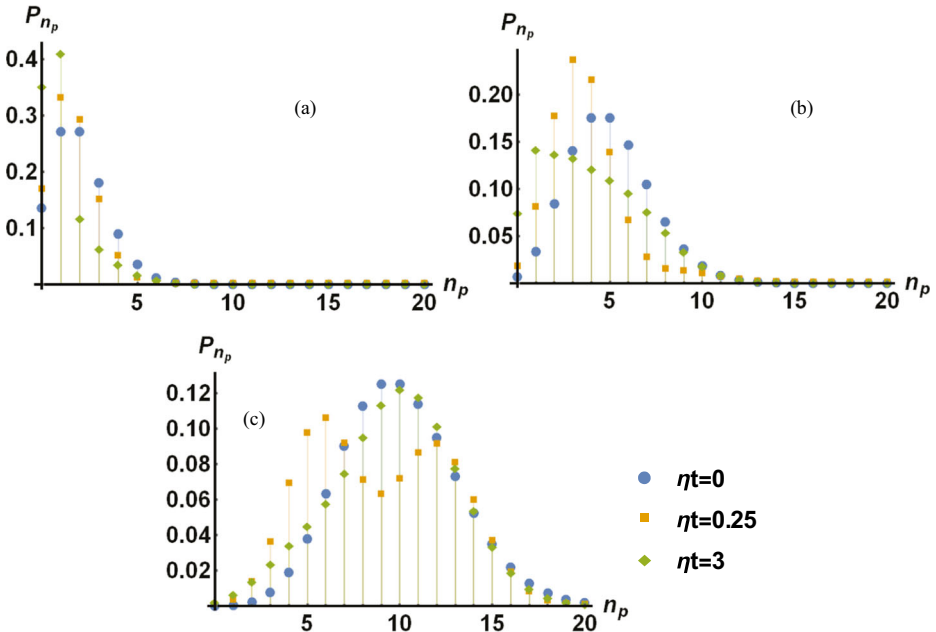


Fig. 7 (Color online) Behavior of photon number distribution P_{n_p} at time $\eta t = 0, 0.25, 3$ for an initially coherent state $|\alpha\rangle$ with $|\alpha| = \sqrt{\bar{n}}$ when (a) $\bar{n} = 2$, (b) $\bar{n} = 5$, (c) $\bar{n} = 10$, respectively

5.2.2 Mean Photon Number and Second-Order Autocorrelation Function

From (46), we have

$$\begin{aligned} \langle a^\dagger a \rangle_{\rho_F(t)} &= |C_1|^2 + \sum_{n=2}^{\infty} |C_n|^2 n \cos^2(\sqrt{n(n-1)}\eta t) \\ &\quad + \sum_{n=2}^{\infty} |C_n|^2 (n-2) \sin^2(\sqrt{n(n-1)}\eta t), \end{aligned} \tag{48}$$

and

$$\begin{aligned} \langle a^{\dagger 2} a^2 \rangle_{\rho_F(t)} &= \sum_{n=2}^{\infty} |C_n|^2 (n-2)(n-3) \sin^2(\sqrt{n(n-1)}\eta t) \\ &\quad + \sum_{n=2}^{\infty} |C_n|^2 n(n-1) \cos^2(\sqrt{n(n-1)}\eta t). \end{aligned} \tag{49}$$

In Fig. 8, we plot $\langle a^\dagger a \rangle$ and $g^{(2)}$ versus ηt for an initial coherent state with different \bar{n} . Obviously, the mean photon number almost do not change over time, accompanying by slight fluctuations. The second-order correlation function is changing up and down in the vicinity of the value 1, i.e. that of the original coherent state. Besides, if the value of \bar{n} is large enough, $g^{(2)}$ is just equal to 1.

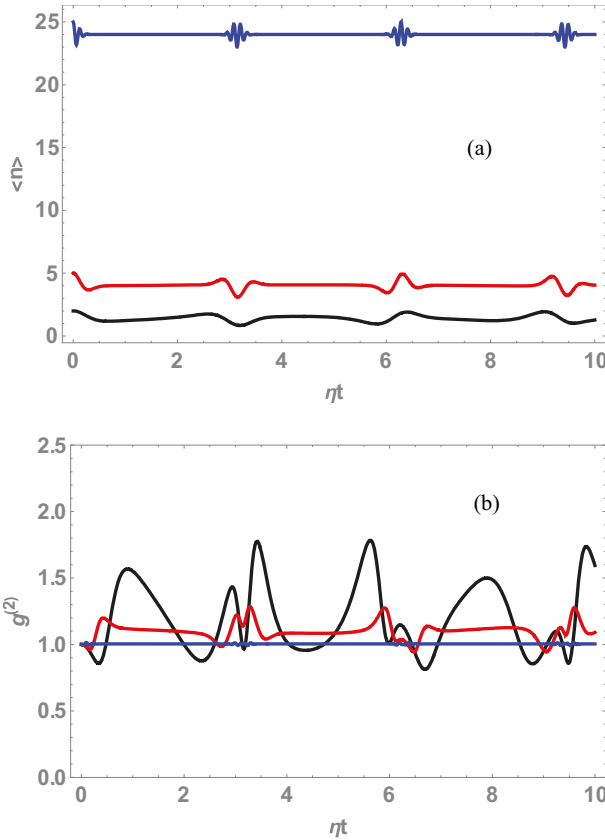


Fig. 8 (Color online) (a) Mean photon number and (b) second-order correlation function $g^{(2)}$ of the optical field as a function of the time ηt , where atom is initially in the ground state $|g\rangle$ and the field is initially in a coherent state $|\alpha\rangle$ with $|\alpha| = \sqrt{\bar{n}}$ ($\bar{n} = 2, 5, 25$ are corresponding to the black, red, and blue line, respectively)

5.2.3 Wigner Function

The Wigner function of the coherent state $|\alpha\rangle$ can be expressed as

$$WF(\xi) = \frac{2}{\pi} \exp(-2|\alpha - \xi|^2), \tag{50}$$

who is a Gaussian function and have no chance to take negative region in phase space. After the interaction, the Wigner function is evolved into

$$\begin{aligned} WF_{\rho_F}(\xi, t) = & |C_0|^2 WF_{|0\rangle\langle 0|}(\xi) + |C_1|^2 WF_{|1\rangle\langle 1|}(\xi) + 2 \operatorname{Re}(C_0 C_1^* WF_{|0\rangle\langle 1|}(\xi)) \\ & + 2 \operatorname{Re}\left(\sum_{n=2}^{\infty} C_n C_0^* \cos(\sqrt{n(n-1)}\eta t) WF_{|n\rangle\langle 0|}(\xi)\right) \\ & + 2 \operatorname{Re}\left(\sum_{n=2}^{\infty} C_n C_1^* \cos(\sqrt{n(n-1)}\eta t) WF_{|n\rangle\langle 1|}(\xi)\right) \end{aligned}$$

$$\begin{aligned}
 & + \sum_{n=2}^{\infty} \sum_{m=2}^{\infty} C_n C_m^* \sin(\sqrt{n(n-1)}\eta t) \sin(\sqrt{m(m-1)}\eta t) W F_{|n-2\rangle\langle m-2|}(\xi) \\
 & + \sum_{n=2}^{\infty} \sum_{m=2}^{\infty} C_n C_m^* \cos(\sqrt{n(n-1)}\eta t) \cos(\sqrt{m(m-1)}\eta t) W F_{|n\rangle\langle m|}(\xi). \tag{51}
 \end{aligned}$$

However, the Wigner function evolved from the initial coherent state can take negative values in some regions of the phase space, as shown in Fig. 9.

It should be noted that, since the infinite series in above expressions cannot be summed exactly in these cases, we will cut the sum superior in a certain number in our numerical analysis. This will lead to some deviation, but will not affect the analysis results.

6 Dynamics Evolution for Initial Case III: $\rho(0) = |g\rangle\langle g| \otimes \rho_{th}$

Assuming the atom initially in the ground state $|g\rangle$ and the field initially in a thermal state ρ_{th} (a mixed state), i.e.

$$\rho(0) = |g\rangle\langle g| \otimes \rho_{th} \tag{52}$$

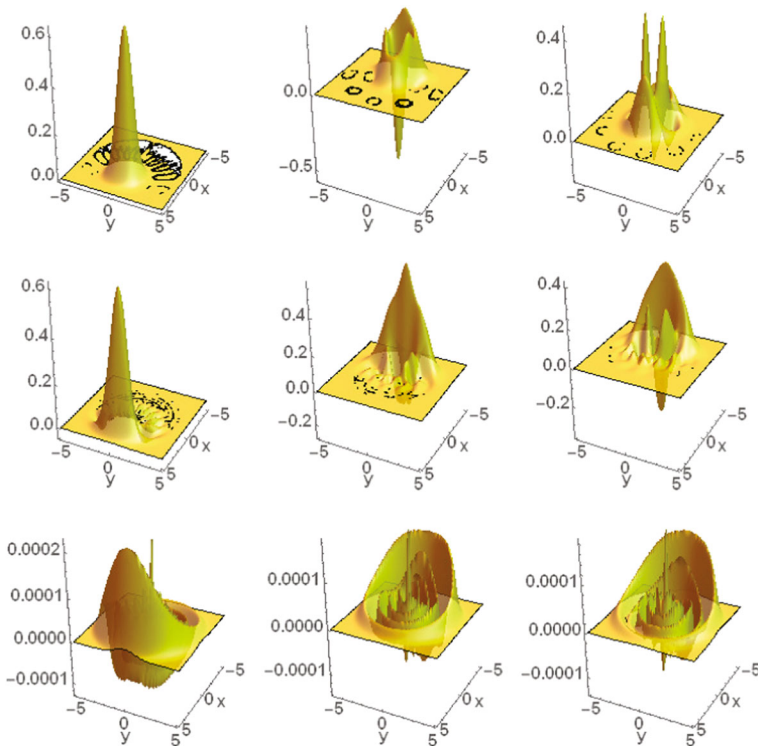


Fig. 9 (Color online) Wigner functions as a function of $\zeta = x + iy$ ($x, y \in [-5, 5]$) for quantum states $\rho_F(t)_{|\bar{n}=2}$ (row 1), $\rho_F(t)_{|\bar{n}=5}$ (row 2), and $\rho_F(t)_{|\bar{n}=25}$ (row 3) and different time scales $\eta t = 0.02$ (column 1), 0.25 (column 2), and 10 (column 3), where atom is initially in the ground state $|g\rangle$ and the field is initially in a coherent state $|\alpha\rangle$ with $|\alpha| = \sqrt{\bar{n}}$ ($\bar{n} = 2, 5, 25$ are corresponding to the black, red, and blue line, respectively)

with

$$\rho_{th} = \sum_{n=0}^{\infty} \frac{\bar{n}^n}{(\bar{n} + 1)^{n+1}} |n\rangle \langle n|, \tag{53}$$

where \bar{n} is the mean photon number of the thermal state, that is

$$\rho_{AF}(0) = \sum_{n=0}^{\infty} \frac{\bar{n}^n}{(\bar{n} + 1)^{n+1}} |g, n\rangle \langle g, n|, \tag{54}$$

then the density operator for times $t > 0$ is just given by

$$\rho_{AF}(t) = \sum_{n=0}^{\infty} \frac{\bar{n}^n}{(\bar{n} + 1)^{n+1}} \exp\left(-\frac{i}{\hbar} H_{eff} t\right) |g, n\rangle \langle g, n| \exp\left(\frac{i}{\hbar} H_{eff} t\right). \tag{55}$$

Through (5) and (10), we easily obtain the total atom-field density operator

$$\begin{aligned} \rho_{AF}(t) &= \frac{1}{\bar{n} + 1} |g, 0\rangle \langle g, 0| + \frac{\bar{n}}{(\bar{n} + 1)^2} |g, 1\rangle \langle g, 1| \\ &+ \sum_{n=2}^{\infty} \frac{\bar{n}^n}{(\bar{n} + 1)^{n+1}} \sin^2(\sqrt{n(n-1)}\eta t) |e, n-2\rangle \langle e, n-2| \\ &- i \sum_{n=2}^{\infty} \frac{\bar{n}^n}{(\bar{n} + 1)^{n+1}} \frac{\sin(2\sqrt{n(n-1)}\eta t)}{2} |e, n-2\rangle \langle g, n| \\ &+ i \sum_{n=2}^{\infty} \frac{\bar{n}^n}{(\bar{n} + 1)^{n+1}} \frac{\sin(2\sqrt{n(n-1)}\eta t)}{2} |g, n\rangle \langle e, n-2| \\ &+ \sum_{n=2}^{\infty} \frac{\bar{n}^n}{(\bar{n} + 1)^{n+1}} \cos^2(\sqrt{n(n-1)}\eta t) |g, n\rangle \langle g, n|. \end{aligned} \tag{56}$$

6.1 Properties of Atom for Initial Case III

The reduced density operator for atom is

$$\begin{aligned} \rho_A(t) &= \left(\frac{1}{\bar{n} + 1} + \frac{\bar{n}}{(\bar{n} + 1)^2} \right) |g\rangle \langle g| \\ &+ \sum_{n=2}^{\infty} \frac{\bar{n}^n}{(\bar{n} + 1)^{n+1}} \sin^2(\eta\sqrt{n-1}\sqrt{nt}) |e\rangle \langle e| \\ &+ \sum_{n=2}^{\infty} \frac{\bar{n}^n}{(\bar{n} + 1)^{n+1}} \cos^2(\eta\sqrt{n-1}\sqrt{nt}) |g\rangle \langle g|, \end{aligned} \tag{57}$$

leading to

$$\begin{aligned} P_e(t) &= \sum_{n=2}^{\infty} \frac{\bar{n}^n}{(\bar{n} + 1)^{n+1}} \sin^2(\sqrt{n(n-1)}\eta t), \\ P_g(t) &= \frac{1}{\bar{n} + 1} + \frac{\bar{n}}{(\bar{n} + 1)^2} \\ &+ \sum_{n=2}^{\infty} \frac{\bar{n}^n}{(\bar{n} + 1)^{n+1}} \cos^2(\sqrt{n(n-1)}\eta t), \end{aligned} \tag{58}$$

and

$$W(t) = - \sum_{n=2}^{\infty} \frac{\bar{n}^n}{(\bar{n} + 1)^{n+1}} \cos(2\sqrt{n(n-1)}\eta t) - \frac{1}{\bar{n} + 1} - \frac{\bar{n}}{(\bar{n} + 1)^2}. \tag{59}$$

In Fig. 10, we plot $P_e(t)$, $P_g(t)$, $W(t)$ versus ηt for a thermal field containing different \bar{n} . In this case, we don't find the phenomena of the quantum Rabi Oscillations found in Case I or the collapse or revival found in case II. In addition, as \bar{n} increases, the atom has a tendency of populating in the excited state and the ground state with equal possibility.

6.2 Properties of Field for Initial Case III

The reduced density operator for the field in case III is

$$\begin{aligned} \rho_F(t) &= \frac{1}{\bar{n} + 1} |0\rangle \langle 0| + \frac{\bar{n}}{(\bar{n} + 1)^2} |1\rangle \langle 1| \\ &+ \sum_{n=2}^{\infty} \frac{\bar{n}^n}{(\bar{n} + 1)^{n+1}} \sin^2(\sqrt{n(n-1)}\eta t) |n-2\rangle \langle n-2| \\ &+ \sum_{n=2}^{\infty} \frac{\bar{n}^n}{(\bar{n} + 1)^{n+1}} \cos^2(\sqrt{n(n-1)}\eta t) |n\rangle \langle n|. \end{aligned} \tag{60}$$

6.2.1 Photon Number Distribution

The photon number distribution for this case can be expressed as follows

$$\begin{aligned} P_0(t) &= \frac{1}{\bar{n} + 1} + \frac{\bar{n}^2}{(\bar{n} + 1)^3} \sin^2(\sqrt{2}\eta t), \\ P_1(t) &= \frac{\bar{n}}{(\bar{n} + 1)^2} + \frac{\bar{n}^3}{(\bar{n} + 1)^4} \sin^2(\sqrt{6}\eta t), \\ P_{n_p}(t) &= + \frac{\bar{n}^{n_p+2}}{(\bar{n} + 1)^{n_p+3}} \sin^2(\sqrt{(n_p + 1)(n_p + 2)}\eta t) \\ &+ \frac{\bar{n}^{n_p}}{(\bar{n} + 1)^{n_p+1}} \cos^2(\sqrt{n_p(n_p - 1)}\eta t), \end{aligned} \tag{61}$$

$(n_p \geq 2).$

In Fig. 11, $P_{n_p}(t)$ for initial thermal states with different \bar{n} are plotted at different time ηt . As \bar{n} increases, the distribution becomes wider. Moreover, the distribution will exhibit oscillation at certain time.

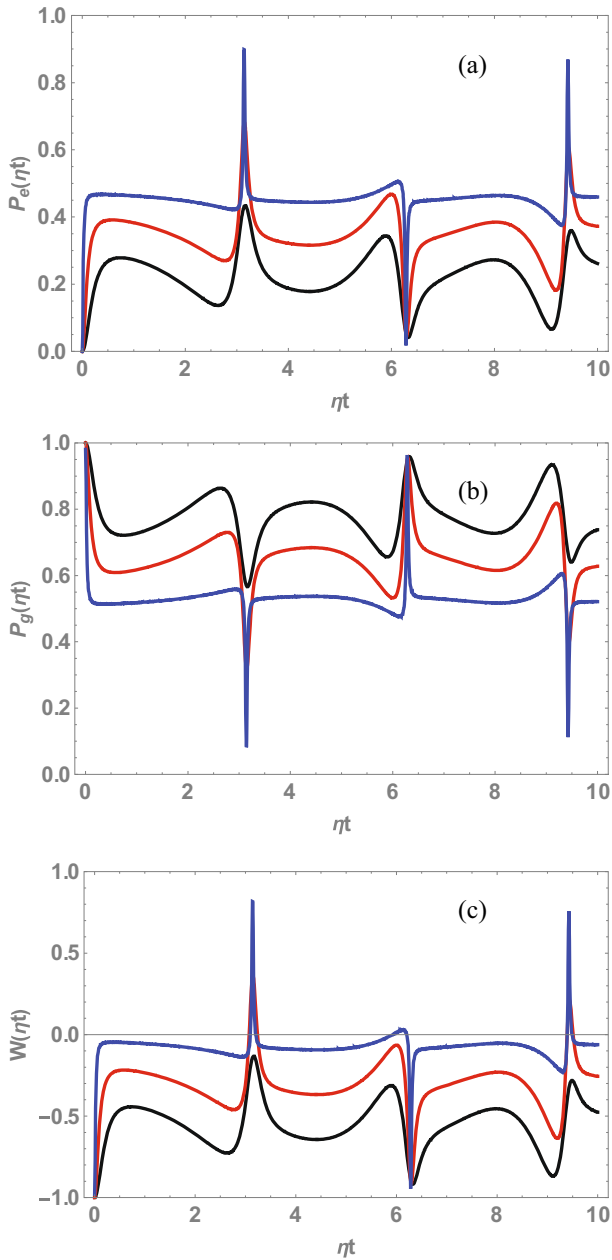


Fig. 10 (Color online) (a) Population in the excited state P_e , (b) Population in the ground state P_g and (c) Atomic inversion W as a function of the time ηt , where atom is initially in the ground state $|g\rangle$ and the field is initially in a thermal state ρ_{th} with the mean photon number \bar{n} . Here $\bar{n} = 2, 5, 25$ are corresponding to the black, red, and blue line, respectively

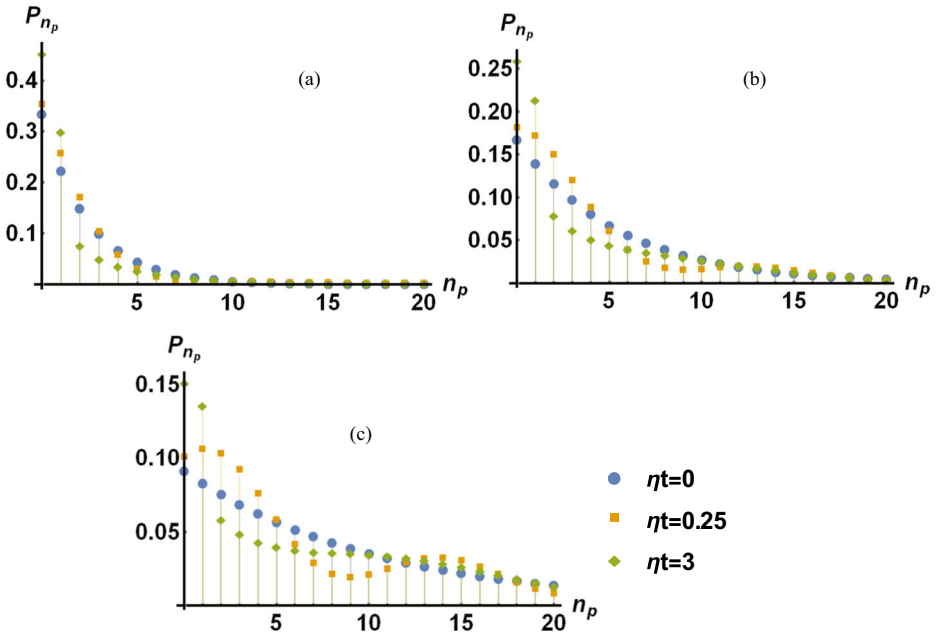


Fig. 11 (Color online) Behavior of $P_{n_p}(t)$ at time $\eta t = 0, 0.25, 3$ for an initial thermal state ρ_{th} with the mean photon number \bar{n} when (a) $\bar{n} = 2$, (b) $\bar{n} = 5$, (c) $\bar{n} = 10$

6.2.2 Mean Photon Number and Second-Order Autocorrelation Function

From (60), we have

$$\begin{aligned}
 \langle a^\dagger a \rangle_{\rho_F(t)} &= \frac{\bar{n}}{(\bar{n} + 1)^2} + \sum_{n=2}^{\infty} \frac{\bar{n}^n}{(\bar{n} + 1)^{n+1}} n \cos^2(\sqrt{n(n-1)}\eta t) \\
 &\quad + \sum_{n=2}^{\infty} \frac{\bar{n}^n}{(\bar{n} + 1)^{n+1}} (n-2) \sin^2(\sqrt{n(n-1)}\eta t), \tag{62}
 \end{aligned}$$

and

$$\begin{aligned}
 \langle a^{\dagger 2} a^2 \rangle_{\rho_F(t)} &= \sum_{n=2}^{\infty} \frac{\bar{n}^n}{(\bar{n} + 1)^{n+1}} (n-2)(n-3) \sin^2(\sqrt{n(n-1)}\eta t) \\
 &\quad + \sum_{n=2}^{\infty} \frac{\bar{n}^n}{(\bar{n} + 1)^{n+1}} n(n-1) \cos^2(\sqrt{n(n-1)}\eta t). \tag{63}
 \end{aligned}$$

In Fig. 12, we plot $\langle a^\dagger a \rangle$ and $g^{(2)}$ versus ηt for an initial thermal state with different \bar{n} . Obviously, the mean photon number almost do not change over time. The second-order correlation function is slightly bigger or equal to 2, i.e. that of the original thermal state.

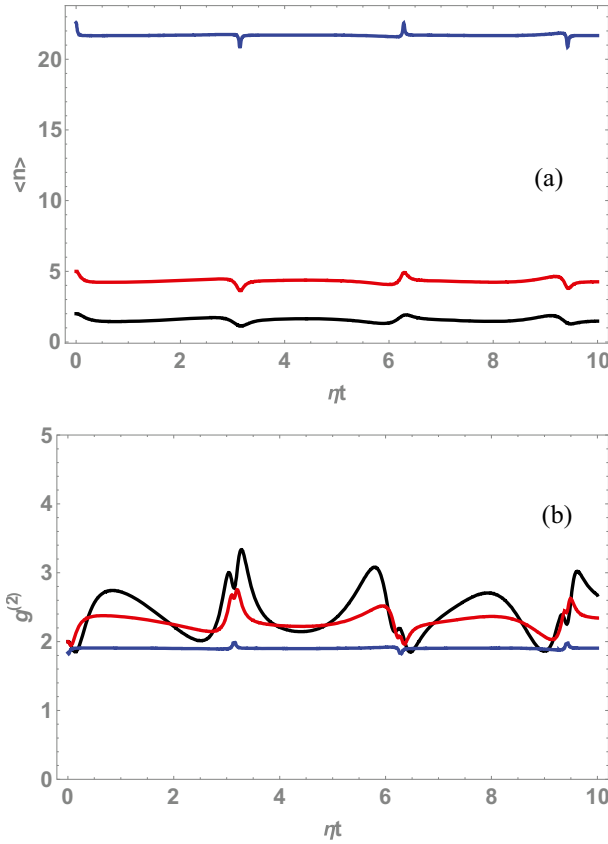


Fig. 12 (Color online) **(a)** Mean photon number and **(b)** second-order correlation function $g^{(2)}$ of the optical field as a function of the time ηt , where atom is initially in the ground state $|g\rangle$ and the field is initially in a thermal state ρ_{th} with the mean photon number \bar{n} . Here $\bar{n} = 2, 5, 25$ are corresponding to the black, red, and blue line, respectively

6.2.3 Wigner Function

The Wigner function of the thermal state ρ_{th} can be expressed as

$$WF(\xi) = \frac{2}{\pi(2\bar{n} + 1)} \exp\left(-\frac{2|\xi|^2}{2\bar{n} + 1}\right). \tag{64}$$

It is also the Gaussian function and has no chance to take negative region in phase space. The Wigner function of $\rho_F(t)$ in case III is written as

$$\begin{aligned} WF_{\rho_F(t)}(\xi, t) &= \frac{1}{\bar{n} + 1} WF_{|0\rangle\langle 0|}(t) + \frac{\bar{n}}{(\bar{n} + 1)^2} WF_{|1\rangle\langle 1|}(\xi) \\ &+ \sum_{n=2}^{\infty} \frac{\bar{n}^n}{(\bar{n} + 1)^{n+1}} \sin^2(\sqrt{n(n-1)}\eta t) WF_{|n-2\rangle\langle n-2|}(\xi) \\ &+ \sum_{n=2}^{\infty} \frac{\bar{n}^n}{(\bar{n} + 1)^{n+1}} \cos^2(\sqrt{n(n-1)}\eta t) WF_{|n\rangle\langle n|}(\xi). \end{aligned} \tag{65}$$

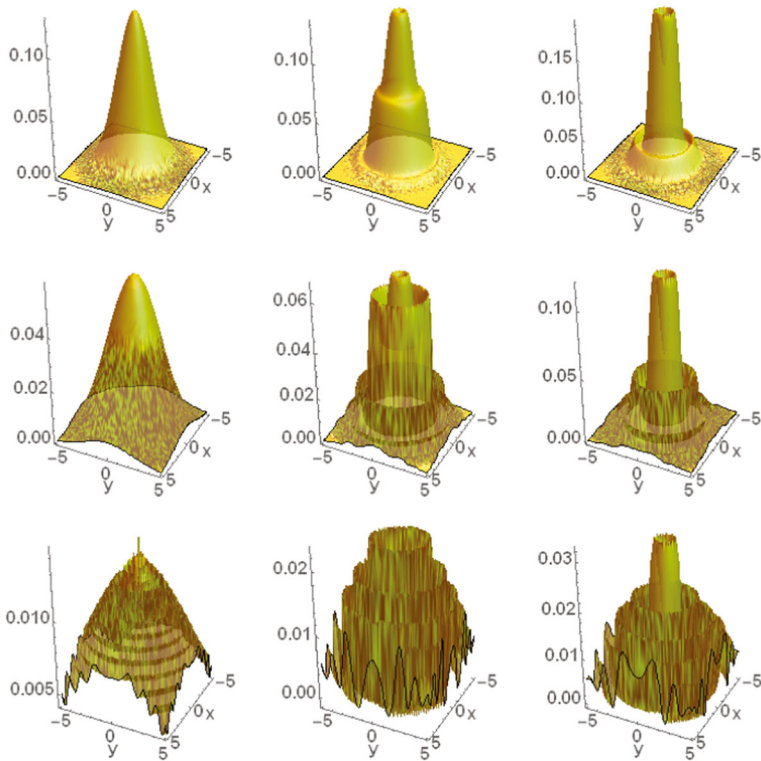


Fig. 13 (Color online) Wigner functions as a function of $\zeta = x + iy$ ($x, y \in [-5, 5]$) for quantum states $\rho_F(t) |_{\bar{n}=2}$ (row 1), $\rho_F(t) |_{\bar{n}=5}$ (row 2), and $\rho_F(t) |_{\bar{n}=25}$ (row 3) and different time scales $\eta t = 0.02$ (column 1), 0.25 (column 2), and 10 (column 3), where atom is initially in the ground state $|g\rangle$ and the field is initially in a thermal state ρ_{th} with the mean photon number \bar{n} . Here $\bar{n} = 2, 5, 25$ are corresponding to the black, red, and blue line, respectively

As Fig. 13 shows, the Wigner function loses the character of Gaussian form and appears some shock in phase space.

7 Conclusion

In summary, we study the dynamical evolution of the properties for the atoms and the fields in the process of two-photon absorption and emission between two atomic levels. Using the eigenstates of the effective Hamiltonian describing the process, we construct the connection between the dressed state and the bare state. Thus we cleverly obtain the density operator of the system at any time once the initial density operator is known. Through the paper, we discuss three cases of initial density operator for the atom-field system, i.e. the atom is initially in the ground state and the optical field is initially in Fock state, coherent state and thermal state, respectively.

For every property under consideration, we give the explicit analytical expressions and make the numerical simulation. Some interesting results are obtained. The phenomenon of quantum Rabi oscillation and collapse and revival for the atom will appear when the proper

initial optical field is injected. This character is similar to that in Jaynes-Cummings model. However, one main difference is that the factor in our model is $\sqrt{n(n-1)}\eta t$ and the factor in Jaynes-Cummings model is $\sqrt{n}\eta t$. In addition, some new optical fields can be generated in our considered process. For instance, after injecting Fock state $|n\rangle$ in the process, we generate the incoherent superposition state of $|n-2\rangle$ and $|n\rangle$, whose ratio can be adjusted by the interaction time. So this process is also effective in the quantum state engineering.

Appendix: Wigner function for the operator $|n\rangle\langle m|$

Substituting

$$\begin{aligned} \langle m| &= \frac{1}{\sqrt{m!}} \frac{d^m}{d\mu^m} \langle 0| \exp(\mu a) |_{\mu=0}, \\ |n\rangle &= \frac{1}{\sqrt{n!}} \frac{d^n}{dv^n} \exp(va^\dagger) |0\rangle |_{v=0}, \end{aligned} \quad (\text{A1})$$

into (17), we have

$$WF_{|n\rangle\langle m|}(\xi) = \frac{2}{\pi \sqrt{m!n!}} \frac{d^{m+n}}{d\mu^m dv^n} \langle 0| \exp(\mu a) : \exp(-2(a^\dagger - \xi^*)(a - \xi)) : \exp(va^\dagger) |0\rangle |_{\mu=v=0}. \quad (\text{A2})$$

Inserting the completeness of the coherent states, i.e. $\int \frac{d^2z_1}{\pi} |z_1\rangle\langle z_1| = 1$ and $\int \frac{d^2z_2}{\pi} |z_2\rangle\langle z_2| = 1$, we have

$$\begin{aligned} WF_{|n\rangle\langle m|}(\xi) &= \frac{2}{\pi \sqrt{m!n!}} e^{-2|\xi|^2} \frac{d^{m+n}}{d\mu^m dv^n} \\ &\times \int \frac{d^2z_1}{\pi} \exp(-|z_1|^2 + \mu z_1 + 2\xi z_1^*) \\ &\times \int \frac{d^2z_2}{\pi} \exp(-|z_2|^2 + (2\xi^* - z_1^*)z_2 + v z_2^*) |_{\mu=v=0}. \end{aligned} \quad (\text{A3})$$

After employing the integration, we obtain the Wigner function for the operator $|n\rangle\langle m|$,

$$WF_{|n\rangle\langle m|}(\xi) = \frac{2 \exp(-2|\xi|^2)}{\pi \sqrt{m!n!}} \frac{d^{m+n}}{d\mu^m dv^n} \exp(+2\mu\xi + 2v\xi^* - \mu v) |_{\mu=v=0}. \quad (\text{A4})$$

Using this expression, the Wigner function for any quantum state can be expressed based on its expansion in Fock state space.

References

1. Scully, M.O., Zubairy, M.S.: Quantum Optics. Cambridge University Press, Cambridge (1997)
2. Walls, D.F., Milburn, G.J.: Quantum optics. Springer, Berlin (2008)
3. Orszag, M.: Quantum optics. Springer, Berlin (2008)
4. Gerry, C.C., Knight, P.: Introductory Quantum Optics. Cambridge University Press, Cambridge (2005)
5. Barnett, S.M., Radmore, P.M.: Methods in Theoretical Quantum Optics. Clarendon Press, Oxford (1997)
6. Haroche, S., Raimond, J.M.: Exploring the quantum: Atoms, Cavities and Photons. Oxford University Press, Oxford (2006)
7. Meystre, P., Sargent, M. III.: Element of quantum optics. Springer, Berlin (2007)
8. Cohen-Tannoudji, C., Dupont-Roc, J., Grynberg, G.: Atom-Photon Interactions. Wiley, New York (1992)

9. Weissbluth, M.: *Photon-Atom Interactions*. Academic Press, New York (1989)
10. Allen, L., Eberly, J.H.: *Optical Resonance and Two-Level Atoms*. Wiley, New York (1975)
11. Eberly, J.H., Narozhny, N.B., Sanchez-Mondragon, J.J.: *Phys. Rev. Lett.* **44**, 1323–1326 (1980)
12. Narozhny, N.B., Sanchez-Mondragon, J.J., Eberly, J.H.: *Phys. Rev. A* **23**, 236–247 (1981)
13. Jaynes, E.T., Cummings, F.W.: *Proc. Inst. Elect. Eng.* **51**, 89–109 (1963)
14. Cummings, F.W.: *Phys. Rev.* **149**, A1051–A1056 (1965)
15. Knight, P.L., Radmore, P.M.: *Phys. Rev. A* **26**, 676–679 (1982)
16. Rabi, I.I.: *Phys. Rev.* **51**, 652–654 (1937)
17. Dell’Anno, F., De Siena, S., Illuminati, F.: *Phys. Rep.* **428**, 53–168 (2006)
18. Yoo, H.J., Eberly, J.H.: *Phys. Rep.* **118**, 239–337 (1985)
19. Shore, B.W., Knight, P.L.: *J. Mod. Opt.* **40**, 1195–1238 (1993)
20. Messina, A., Maniscalco, S., Napoli, A.: *J. Mod. Opt.* **50**, 1–49 (2003)
21. Schleich, W.P.: *Quantum Optics in Phase Space*. Wiley-Vch Verlag, Berlin (2001)
22. Knight, P.L., Milonni, P.W.: *Phys. Rep.* **66**, 21–107 (1980)
23. Allen, L., Knight, P.L.: *Concepts of Quantum Optics*. Pergamon, Oxford (1983)
24. Wigner, E.P.: *Phys. Rev.* **40**, 749–759 (1932)